ENVIRONMENTAL RESEARCH
LETTERS

LETTER • **OPEN ACCESS**

Particulate dominance of organic carbon mobilization from thaw slumps on the Peel Plateau, NT: Quantification and implications for stream systems and permafrost carbon release

To cite this article: S Shakil *et al* 2020 *Environ. Res. Lett.* **15** 114019

Environmental Research Letters

LETTER

Particulate dominance of organic carbon mobilization from thaw slumps on the Peel Plateau, NT: Quantification and implications for stream systems and permafrost carbon release

S Shakil[1], S E Tank[1], S V Kokelj[2], J E Vonk[3] and S Zolkos[1,4]

[1] Biological Sciences, University of Alberta, Edmonton, Canada
[2] Northwest Territories Geological Survey, Yellowknife, NT X1A 2L9, Canada
[3] Department of Earth Sciences, Vrije Universiteit, Amsterdam, The Netherlands
[4] current address: Woods Hole Research Center, Falmouth, MA 02540, United States of America

E-mail: shakil@ualberta.ca

Keywords: thermokarst, climate change, permafrost, organic carbon, particulate, streams

Supplementary material for this article is available online

OPEN ACCESS

RECEIVED
12 May 2020

REVISED
21 July 2020

ACCEPTED FOR PUBLICATION
4 August 2020

PUBLISHED
27 October 2020

Abstract

Climate change is increasing the frequency and intensity of thermokarst, and accelerating the delivery of terrestrial organic material from previously sequestered sources to aquatic systems, where it is subject to further biochemical alteration. Rapid climate change in the glacially conditioned ice-rich and ice-marginal terrain of the Peel Plateau, western Canada, is accelerating thaw-driven mass wasting in the form of retrogressive thaw slumps, which are rapidly increasing in area, volume and thickness of permafrost thawed. Despite major perturbation of downstream sedimentary and geochemical fluxes, few studies have examined changes in flux and composition of particulate organic carbon (POC) in streams and rivers as a result of permafrost thaw. Here we show that the orders of magnitude increase in total organic carbon, nitrogen, and phosphorus mobilized to streams from thaw slumps on the Peel Plateau is almost entirely due to POC and associated particulate nitrogen and phosphorus release. Slump-mobilized POC is compositionally distinct from its dissolved counterpart and appears to contain relatively greater amounts of degraded organic matter, as inferred from base-extracted fluorescence of particulate organic matter. Thus, slump-mobilized POC is potentially more recalcitrant than POC present in non-slump affected stream networks. Furthermore a substantial portion of POC mobilized from thaw slumps will be constrained within primary sediment stores in valley bottoms, where net accumulation is currently exceeding net erosion, resulting in century to millennial scale sequestration of thermokarst-mobilized POC. This study highlights the pressing need for better knowledge of sedimentary cascades, mobilization, and storage reservoirs in slump-affected streams, and baseline assessments of the biodegradability of POC and cycling of particulate nutrients within a sedimentary cascade framework. Explicit incorporation of POC dynamics into our understanding of land-water carbon mobilization in the face of permafrost thaw is critical for understanding implications of thermokarst for regional carbon cycling and fluvial ecosystems.

1. Introduction

Abrupt climate-driven permafrost thaw (i.e. thermokarst) is prevalent across the circumpolar north (Olefeldt *et al* 2016, Kokelj *et al* 2017a) and is accelerating in ice-rich glaciated landscapes (Segal *et al* 2016, Lewkowicz and Way 2019). Degradation of ice-rich ground liberates sequestered materials, saturates thawing soils and sediments, and enables mixing of various soil layers that may substantially differ in composition (Vonk *et al* 2015, Kokelj *et al* 2015, Lacelle *et al* 2019). Thermokarst on slopes can rapidly translocate large volumes (10^2 to 10^6 m^3) of previously frozen materials downslope (Kokelj *et al* 2015, van der Sluijs *et al* 2018) to new storage reservoirs in valley bottoms where material is subject to

fluvial erosion and entrainment (Kokelj *et al* 2013), thereby exposing material to light, dissolution, and microbial degradation (Vonk *et al* 2015).

The growing need to include thermokarst processes (Kokelj and Jorgenson 2013) into Earth system or land surface models (Turetsky *et al* 2020) has advanced research on quantifying carbon storage in thermokarst landscapes (Olefeldt *et al* 2016, Fuchs *et al* 2018, 2019) and measuring carbon fluxes and composition from thermokarst features (Vonk *et al* 2015, Littlefair *et al* 2017, Tanski *et al* 2017, Ramage *et al* 2018). However, studies on organic carbon mobilization from thermokarst features have predominantly focused on dissolved organic carbon (DOC) (e.g. Mann *et al* 2015, Abbott *et al* 2015, Littlefair *et al* 2017), with effects varying from orders of magnitude increases in concentrations (Manning *et al* 2015) to little response or a decrease in concentrations (Littlefair *et al* 2017) due to a combination of landscape state factors that control organic matter accumulation in permafrost and its release (Ewing *et al* 2015, Mu *et al* 2017, Tank *et al* 2020). Most work examining thermokarst-mobilized particulate organic carbon (POC) flux has focused on coastal erosion (Vonk *et al* 2012, Tanski *et al* 2017, Ramage *et al* 2018), and studies detecting signatures of permafrost thaw in major northern rivers (Guo and Macdonald 2006, Guo *et al* 2007, Wild *et al* 2019, Bröder *et al* 2020), the latter of which have noted POC is more aged than dissolved or colloidal phases, thus reflecting a greater degree of mobilization from deeper permafrost deposits. Although work on Melville Island has shown that active layer detachments can increase the delivery of aged POC to stream networks (Lamoureux and Lafreniere 2014, Beel *et al* 2020), studies on POC mobilization in fluvial systems is extremely limited.

Organic matter is a vital source of energy and nutrients to the microbial base of aquatic food webs (Manning *et al* 2015). The composition of organic matter, such as its C: N: P stoichiometry, molecular structure, and degree of mineral association, can impact the relative importance of carbon transfer through food webs, relative to mineralization to CO_2 (Sardans *et al* 2012, Manning *et al* 2015, Welti *et al* 2017). Thermokarst may alter the relative abundance of organic matter from different sources (Wauthy *et al* 2018) and phases (particulate vs. dissolved) in recipient systems. If sources of organic carbon differ substantially in their composition, then rapid transfer of terrestrial material via thermokarst processes may have the potential to abruptly alter energy transfer to and through aquatic systems. 'Autochthonous' organic matter, derived from living material in the stream channel (e.g. algae) is generally considered to be more labile and of greater nutritional quality for upper trophic levels than terrestrial organic matter, partly due to the lower carbon-to-nutrient ratios, higher algal polyunsaturated fatty-acid content, and the complex amorphous structure of terrestrial organic matter (Guo *et al* 2016, Brett *et al* 2017). However, the origin and nature of terrestrial deposits can vary. Lipid degradation proxies have suggested that permafrost-sourced particulate organic matter (POM) in the Kolyma river is more labile than POM in a headwater stream with POM dominated by in-stream production and recent vegetative sources (Bröder *et al* 2020). Pautler *et al* (2010) also found elevated microbial activity in soil organic matter redistributed by active layer detachments on Melville Island, suggesting the release of labile soil organic matter from thawing permafrost. Many studies have found permafrost-derived DOC to be more biodegradable than relatively more modern DOC present in adjacent aquatic systems (Abbott *et al* 2014, Spencer *et al* 2015, Littlefair and Tank 2018). In some landscapes, this elevated lability has been attributed to the preservation and/or accumulation of biolabile compounds in permafrost (Ewing *et al* 2015, Strauss *et al* 2017), while in others it may be due in part to biochemical processes occurring when multiple soil profiles mix prior to delivery to stream systems (Littlefair and Tank 2018). However, the elevated lability of permafrost-derived organic matter is not consistent throughout the Arctic (Burd *et al* 2020, Wickland *et al* 2018) highlighting the need for contextualizing the fate of organic matter mobilized by permafrost thaw in relation to landscape state factors that may control the diagenetic state of terrestrial organic matter and how it is released during thaw (Tank *et al* 2020). But assessments on thermokarst-mobilized organic matter composition and lability are dominantly made for the dissolved phase. Across boreal aquatic ecosystems, POC can have significantly elevated mineralization rates relative to DOC (Attermeyer *et al* 2018), which suggest assessments based on DOC could be inaccurate for total organic carbon pools if POM and associated POC are the dominant form of organic matter and carbon mobilized to recipient aquatic systems.

One of the most dramatic forms of thermokarst is the retrogressive thaw slump (henceforth 'thaw slump'). Thaw slumps occur at high densities in glacially conditioned permafrost landscapes including ice-marginal moraine systems, and glaciofluvial, glaciolacustrine, and glaciomarine deposits (Rudy *et al* 2017, Kokelj *et al* 2017a, Ward Jones *et al* 2019). Thaw slumps develop as ice-rich permafrost thaws and collapses, and saturated materials flow over sloping terrain, transporting material downslope to streams, lakes, or coastal environments. These dynamic thermokarst systems predominantly affect low order streams where they overwhelm transport capacity and can transform long-term sediment flux (Kokelj *et al* 2017a, Kokelj *et al* under review). On the Peel Plateau in the western Canadian Arctic, a warming and wetting climate has intensified thaw slump activity (Kokelj *et al* 2015, Segal *et al* 2016). The region has one of the highest density of large thaw slumps

in northwestern Canada with most features occurring in headwater streams of east-flowing tributaries of the Peel River (Kokelj *et al* 2017a). As thaw slumps erode hillslopes, they can increase sediment loads in streams by orders of magnitude (Kokelj *et al* 2013), and expose materials normally unavailable for transport to stream systems, such as glacial tills maintained in permafrost since the Pleistocene (Lacelle *et al* 2013, 2019). The degree to which thaw slumping changes the nature and quantity of organic matter mobilized to streams may depend on the characteristics of surficial materials and thickness of permafrost thawed, in addition to ground-ice content, topography, and intensity of climate conditions that drive slope thermokarst processes (Kokelj *et al* 2015, 2017a, Lacelle *et al* 2019).

Here, we target three key goals. First, we quantify the relative magnitude of POC vs. DOC mobilization to stream water columns on the Peel Plateau. Second, we assess how thaw slumping affects the source and composition of organic matter present in recipient streams. Third, we examine how changes in the quantity and composition of mobilized organic matter varies in relation to thaw slump morphology and landscape variation. We undertake this work across a series of thaw slump features that vary in their morphology and landscape position as it relates to the nature of materials mobilized by thaw. Assessing POC mobilization and its overall composition is critical to understand and predict the impacts of abrupt permafrost thaw on aquatic ecosystems and carbon cycling, and to advance our understanding of the biogeochemical effects of permafrost thaw within aquatic networks.

2. Methods

2.1. Study region

The Peel Plateau is a 24 000 km^2 glacially conditioned landscape characterized by ice-rich, fluvially incised terrain that is representative of other permafrost preserved glaciated landscapes across northwestern Canada, Alaska, and Siberia (Kokelj *et al* 2017b) (figure 1). The headwaters of east flowing Peel River tributaries originate in mountainous unglaciated terrain where surficial materials are dominated by colluvium, and transition to glacial till with decreasing topographic relief towards the east (Duk-Rodkin and Hughes 1992, Kokelj *et al* 2017b). The transition from tundra to shrub to stunted boreal forest in lowlands is associated with the regional topographic gradient that generally occurs West to East (O'Neill *et al* 2015) and may affect the organic carbon content in active layer and Holocene-age permafrost (Dyke 2005).

The region's ice-rich, fluvially-incised landscape is characterized by a high density of thaw slumps (Segal *et al* 2016) compared to many glaciated permafrost landscapes to the east (Kokelj *et al* 2017b). In the late-Pleistocene (ca. 18, 000 to 15, 000 cal. yr. BP; Lacelle *et al* 2013), the region was briefly covered by the Laurentide Ice Sheet (LIS). During this time, glacial tills, glaciofluvial and glaciolacustrine materials were deposited in a dynamic ice-marginal setting (Lacelle *et al* 2013) and preserved as permafrost was established following glacial retreat (Lacelle *et al* 2004, 2013). Subsequent early Holocene warming was associated with an increase in active layer thickness to ~1.5 fold that of present day conditions (ca. 9000 cal. yrs. BP, Burn *et al* 1997), and an acceleration of mass-wasting (e.g. thaw slumping) and development of colluvial deposits. These processes enabled soil formation, geochemical modification and the incorporation of organics to the depths of maximum thaw, followed by a cooling period and upwards aggradation of the permafrost table (Lacelle *et al* 2019). These modified deposits have been preserved in a 'relict-thaw layer' situated immediately below present-day active layer soils, distinguished from the unmodified tills below by a thaw unconformity (Lacelle *et al* 2019). Thus, the relict-thaw layer can be comprised of a paleo-active layer and/or sediments deposited at the base of a hillslope from past slumping activity (colluvial deposits, Lacelle *et al* 2019).

Considering this history, we refer to three main categories of terrestrial material eroded by thaw slumps: (1) the currrent active layer, where soil has developed from the relict-thaw layer; (2) Holocene-age permafrost containing previously thawed diamicton (relict-active layer) and colluvium (slumped sediments); and (3) Pleistocene-age permafrost containing tills that have remained preserved within permafrost. Headwall height, scar zone area, and debris tongue length (figures 1(a)–(b)) vary by orders of magnitude (table 1, Kokelj et al under review), potentially affecting the relative contributions of different sources exposed in headwalls and their delivery to streams.

2.2. Site selection

Eight thaw slump sites were selected for sampling within the Stony Creek and Vittrekwa River watersheds on the Peel Plateau (figure 1, table 1). Sites were selected based on the following criteria in order of importance: (1) connection of channelized runoff to a stream network; (2) provision of a range of variation in slump morphology; and (3) availability of data from previous studies to build on a baseline body of knowledge (Kokelj *et al* 2013, Littlefair *et al* 2017). This selection was constrained by accessibility of sites due to the remote location of the region. The Stony Creek and Vittrekwa watershed were targeted due to the ability to access sites from the Dempster Highway.

Sites were visited two to three times from June to August 2015. Samples were obtained from: channelized runoff within each thaw slump (IN); a downstream location where all channelized runoff entered the valley-bottom stream (DN); and an unimpacted

Table 1. Maximum headwall heights, slump area, estimated scar volumes, debris tongue volumes, debris tongue lengths, elevation, and maximum scar-valley slope for the eight slump sites included in this study. Delineated watershed areas for the upstream and downstream location at each slump site is also provided. ND indicates no data.

Site	Lat (DD)	Long (DD)	Headwall height[a] (~m, max)	Area[b] (10^4 m^2)	Est. scar vol.[c] (10^4 m^3)	Debris tongue volume[d] (2017, 10^4 m^3)	Debris tongue length[e] (m)	Dist. to late GL (m)	Elevation[f] (m, max)	Max. scar-valley slope (%)	Watershed Area (km^2)	
											UP	DN
FM2	67.25770	−135.23694	25	31.7	240 (600)	195	1529	18 918	373	67	0.73	15.95
SE	67.14862	−135.71803	23	1.5	3.1	ND	30	−3452	576	123	5.33	5.54
FM4	67.27798	−135.15955	17	8.8	38	ND	960	22 901	296	98	3.41	4.35
HD	67.40057	−135.33413	11.7	1.8	4.0	ND	137	23 713	323	65	17.94	18.30
FM3	67.25335	−135.27281	10.3	6.1	23 (50)	14.7	576	17 312	399	34	3.18	3.75
HA	67.15074	−135.68652	7.3	5.9	22	ND	288	−3015	530	80	0.90	1.08
HB	67.24054	−135.82028	7.1	13.6	71	ND	257	−3215	666	35	0.69	1.02
SD	67.18030	−135.72717	2	<1	<1.7	ND	0	−3914	594	67	0.92	1.09

[a]Sources: Zolkos *et al* (2019)

[b]Sources: Littlefair *et al* (2017), SE approximated from Google Earth, based on 2016 imagery

[c]Pre-disturbance scar volume estimated from scar volume vs. scar area relationships, bracketed values show measured values in 2017 [Kokelj et al under review; $\log(\text{vol}) = -1.44 + 1.42(\log(\text{area}))$]

[d]based on 2017 data, van der Sluijs *et al* (2018) and Kokelj et al under review

[e]Sources: Littlefair *et al* (2017); Zolkos *et al* (2018)

[f]Maximum elevation within ~100 m of the headwall (supplementary S9)

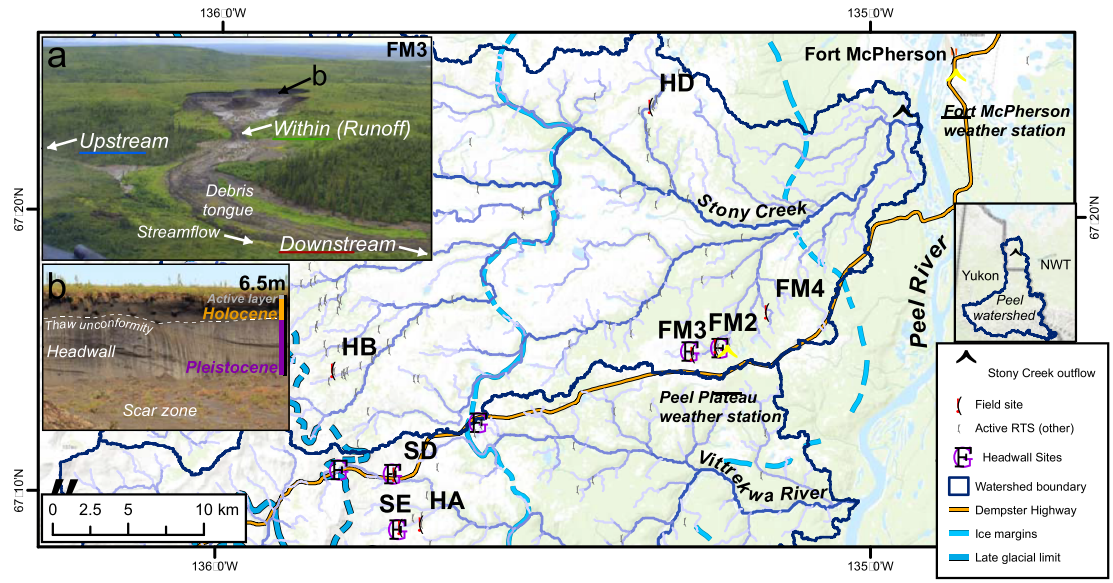

Figure 1. Location of slump sites sampled for stream water chemistry on the Peel Plateau, NWT. Inset (a) shows stream sampling points relative to a slump site. Inset (b) shows headwall units of a slump. Active RTS features are from Segal *et al* (2016). Glacial limits are from Duk-Rodkin and Hughes (1992). Basemap used is ESRI World Topographic Map. Adapted from Zolkos *et al* (2018). John Wiley & Sons. ©2018. American Geophysical Union. All Rights Reserved.

reference stream that was usually directly upstream of the slump inflow (UP). FM2-UP is an exception being an unimpacted tributary flowing into the downstream sampling point, but not directly upstream. Given the requirement for unimpacted upstream sites, all sites are located on independent subcatchments with the exception that FM2-DN is downstream of FM3-DN. Downstream locations typically integrated channelized runoff and materials entrained by channel erosion of the debris tongue, along with potentially enhanced sideslope erosion (Kokelj *et al* 2015, van der Sluijs *et al* 2018).

2.3. Stream sample collection

Water samples were collected in pre-acid-leached high-density polyethylene (HDPE) bottles or DI-leached low-density polyethylene (LDPE) cubitainers when greater volumes were needed for suspended particulate parameters. Both containers were triple sample-rinsed. Due to high sediment loads, water samples for dissolved constituents were allowed to settle for ~24 h prior to vacuum filtration (following Littlefair *et al* 2017) through pre-combusted glass fibre filters (Whatman, GF/F, 0.7 μm). Dissolved constituents included DOC, total dissolved nitrogen (TDN) and phosphorus (TDP), dissolved inorganic nitrogen (DIN: NH_4^+ & NO_3^- + NO_2^-), and soluble reactive phosphorus (SRP). Dissolved organic nitrogen (DON; TDN-DIN) and organic phosphorus (DOP; TDP-SRP) were calculated from measured nutrient species. Any DOP concentrations below the limit of quantitation for TDP (4.9 μg l^{-1}) were replaced with half the limit's value (supplementary S1.2). Suspended particulate material was collected on pre-weighed and pre-combusted (450 °C, 5 h) glass fibre filters (Whatman, GF/F) within 24 h of collection and stored frozen for analysis of POC & POδ^{13}C, particulate nitrogen (PN) & Pδ^{15}N, particulate organic phosphorus (POP), and PO^{14}C. PO^{14}C samples were collected from three of our eight sites (FM2, FM3, SD, capturing slump morphology range; table 1) on pre-combusted (500 °C, 5 h) quartz fibre filters (Whatman, QM/A, 2.2 μm). In 2016, sites accessible by foot (5 of 8) were re-visited to obtain samples to measure optical characteristics of base-extracted particulate organic matter (BEPOM) (Osburn *et al* 2012, Brym *et al* 2014). For further details, see supplementary S1.

2.4. Quantification of organic carbon delivery (Goal 1)

We calculated instantaneous yields of POC, DOC, and total organic carbon (TOC) upstream and downstream of thaw slumps using paired measurements of constituent concentration and stream discharge, and watershed areas delineated in ArcGIS (supplementary S4). We determined slump effects on TOC yields with linear mixed effects models using the R package lme4 (Bates *et al* 2015; supplementary S5). We included random slope and random intercept terms, accounting for repeated measures by allowing the slope (i.e. slump effect) and intercept to vary per slump site.

2.5. Source contributions to stream organic carbon (Goal 2)

Stream periphyton and headwall samples were collected at six slump sites in 2017 for POδ^{13}C end member values (supplementary S6). Headwall sources consisted of an upper active layer (O-horizon), lower active layer (resembling A and/or B soil horizons),

and Holocene and Pleistocene permafrost. Headwall samples were additionally analyzed for Pδ^{15}N, and %POC, %PN, and %POP. FM2 and FM3 headwalls were also sampled for PO^{14}C to match 2015 stream PO^{14}C. Contributions of sources to upstream, within, and downstream POC were quantified using a dual carbon (^{13}C, ^{14}C) mixing model (MixSIAR, Stock *et al* 2018; supplementary S7).

2.6. *Assessment of compositional changes in particulate organic material* via *geochemical analyses (Goal 2)*

We used linear mixed effects models (section 2.4) to examine slumping effects on: POC:PN and POC:POP stoichiometry (Sardans *et al* 2012, Manning *et al* 2015); POδ^{13}C and Pδ^{15}N, used as metrics of organic matter source (Finlay and Kendall 2008) and stage of decay (^{13}C enrichment via anaerobic decomposition; Gundelwein *et al* 2007); and percent POC (%POC; as POC:TSS), used as a metric of organic carbon content of sediments. We further examined DOC:DON and DOC:DOP ratios to compare the dissolved and particulate response. We used principal components analysis (PCA) to (a) build upon our linear mixed models and assess broad patterns in geochemical parameters across sites, and (b) compare the geochemical composition of streamwater particulate organic matter (POM) to headwall sources (section 2.5). Variables with highly skewed and non-normal distributions were transformed prior to analysis.

2.7. *Assessments of compositional changes* via *optical analyses of base-extracted particulate organic matter (BEPOM) (Goal 2)*

Absorbance and fluorescence spectra of BEPOM were analysed following Osburn *et al* (2012) and Brym *et al* (2014). We calculated spectral slopes, slope ratios (S_R), and total absorbance from 250–450 nm per unit of suspended sediment ($a_{tot/TSS}$, Helms *et al* 2008, Brym *et al* 2014) as proxies for molecular weight and relative quantity of extractable chromophoric organic matter per unit of sediment. A parallel factor analysis (PARAFAC) model was fit to excitation-emission matrices (drEEM toolbox in MATLAB; Murphy *et al* 2013) to resolve fluorescent components associated with fluorescent organic matter pools with different bulk molecular structure. Relative contribution of components to sample fluorescence was determined by normalizing maximum fluorescence intensities (F_{max}) of each component to the sum of component intensities for a given sample ($\%C = F_{max}/(\sum F_{max})$). Excitation-emission matrices were corrected and smoothed prior to any calculations and modelling. Further details are in supplementary S2. To aid component interpretations, we calculated commonly-used fluorescence indices (table S2), and assessed relationships between these indices and our PARAFAC components using PCA, transforming any highly skewed or non-normal variables (supplementary S3). Follow-up analyses on variables of interest were conducted using repeated measures ANOVA
(supplementary S8).

2.8. Landscape and environmental controls on composition and delivery (Goal 3)

We used a linear model (lm() in R) to examine the relative importance of morphological, meteorological, and landscape effects on variation in upstream vs. within and upstream vs. downstream comparisons (i.e. slump effects) across slump sites. Slump effects were represented by extracting the random slopes per slump site from the aforementioned linear mixed effects models of TOC yield (section 2.4) and %POC (section 2.6, table 2). We ran two separate models for upstream vs. within and upstream vs. downstream random slopes. Explanatory variables consisted of: debris tongue length and maximum headwall height (morphological effects; Littlefair *et al* 2017, Zolkos *et al* 2019); total rainfall over the 96 h preceding sampling (meteorological effects; Kokelj *et al* 2015); and longitude of slump site and stream power immediately downstream of the RTS (landscape effects). Maximum slope across the scar zone to immediate valley bottom was also used as a landscape variable for the TOC yield model. Through our study design we attempted to control meteorogical variation by sampling all sites close in time, but meteorological variables were included to account for the fact that sites were sampled on a series of sequential days. For further details on explanatory variables see supplementary S9.

3. Results

3.1. The effects of slumping on TOC and nutrient delivery to streams (Goal 1)

POC accounted for the majority of organic carbon present within the channelized runoff of slumps. Within-slump POC concentrations reached greater than 9000 mg l^{-1}, while the maximum DOC concentration recorded was 33.6 mg l^{-1}. Within-slump sediment concentrations at some sites (FM2, SE) accounted for 10%–30% of the water volume, further decreasing per-volume DOC estimates and increasing the importance of POC fluxes and yields. Instantaneous total organic carbon (TOC) yields increased, on average, by an order of magnitude downstream of thaw slumps ($p = 0.005$, table 2, figures 2(a) and (d). Increases in POC yields accounted for 85%–100% of TOC increases, except for two out of three instances at SD, where POC accounted for 31% of TOC increases, and in one instance, TOC yield decreased downstream by ~ 6 mg s^{-1} km^{-2} due to decreases in DOC yield (figures 2(a) and (e)). In 43% of our observations, DOC yields decreased downstream of slumps.

Table 2. Results of the linear mixed effects regression models (estimate, error, degrees of freedom [df], t-statistic [t], and p-value [p]) comparing organic matter composition upstream, within, and downstream of thaw slump runoff. Estimate shows the effect of change in stream location (upstream vs. downstream, upstream vs. within-slump) on dependent variables and error shows standard error of the estimate.

	Upstream vs. Downstream					Upstream vs. Within-slump					Random Effects in model
Variable	Estimate	Error	df	t	p	Estimate	Error	df	t	p	
log (TOC yield)	0.9303	0.2374	7.3	3.92	**0.005**			N/A			(1 + StreamLocation|SlumpSite)
log (POC: POP)	−0.0461	0.0725	53.5	−0.636	0.527	0.1215	0.0725	53.5	1.676	**0.010**	(1|SlumpSite)
POC:PN	Not assessed, singular fit warnings for all models										
$(PO\delta^{13}C)^{-1}$	−0.0006	0.0001	53.25	−7.168	**<0.001**	−0.0008	0.0001	53.25	−9.727	**<0.001**	(1|SlumpSite)
$P\delta^{15}N$	Not assessed, singular fit warnings for all models or failure to converge										
$(\%POC)^{-1}$	0.2779	0.0450	7.13	6.189	**<0.001**	0.2140	0.0640	7.06	3.342	**0.012**	(1 + StreamLocation|SlumpSite) + (1|Jday)
log (DOC: DOP)	−0.0381	0.0748	53.6	−0.509	0.613	−0.3676	0.0748	53.6	−4.913	**<0.001**	(1|SlumpSite)
log (DOC: DON)	−0.0844	0.0668	51.5	−1.262	0.213	−0.3515	0.0660	51.4	−5.329	**<0.001**	(1|SlumpSite)

With the exception of site SD, the high concentrations of particles mobilized from within-slump shifted streams from being DOC to POC dominated (figures 2(a), 3(a) and (d).

Increases in suspended sediment delivery and associated PN and POP to streams also led to orders of magnitude increases in instantaneous total nitrogen (as TDN + PN) and phosphorus (as TDP + POP) yields (figures 2(b)–(c), figures 3(b)–(c)). Greater DON and DOP concentrations within slumps relative to upstream did not result in elevated downstream concentrations relative to upstream (figures 3(e)–(f)). Across stream locations, POC:POP ratios were lower than DOC:DOP ratios (figure 3(l)). POC:PN ratios were also lower than DOC:DON and DOC:DIN ratios at all downstream locations with the exception of one sample downstream of SC (figures 3(j)–(k)).

High DIN concentrations within slump runoff did result in elevated concentrations downstream, largely driven by increases in NH_4^+ (figure 3(h)). In contrast, no consistent difference was noted in SRP concentrations (figure 3(i)). TDN:TDP ratios were often more than double the Redfield ratio of 16:1, a guideline for nutrient limitation in marine and freshwater systems (figure 3(g)). With the exception of site SE, ratios were elevated within-slump, relative to upstream sites, sometimes leading to elevated ratios downstream relative to upstream (figure 3(g)).

3.2. The effect of slumping on sources of stream POC and DOC (Goal 2)

Terrestrial sources accounted for upwards of 80% of POC upstream, within, and downstream of sites incorporated in the dual-carbon isotope model (SD, FM2, and FM3, figure 4, table S5). Across all eight sites, upstream POδ^{13}C was variable and sometimes more ^{13}C depleted than active layer sources (figure 5(b)), indicating differing contributions from ^{13}C depleted *in situ* sources (i.e. periphyton, POδ^{13}C $= -33.39 \pm 4.19$, *mean* $\pm$ *SD*) across sites. Slumping increased POC mobilization from both Pleistocene-age and Holocene-age permafrost, but POC from Pleistocene-age permafrost appeared to contribute more on average to within-slump and downstream POC (figure 4(b)). The small permafrost contributions to upstream POC are due to incorporation of FM3-UP in the model, which began to experience streambank erosion and has more ^{14}C-depleted POC than other upstream sites (figure 4(a)). DOδ^{13}C (Zolkos *et al* 2018) and DOΔ^{14}C (Littlefair *et al* 2017) suggest DOC is also predominantly terrestrial, with upstream DOC sourced from O-horizon soils (figure 4(a)). Similar to upstream POδ^{13}C, upstream DOδ^{13}C values were more ^{13}C depleted than within-slump DOδ^{13}C, suggesting relatively greater contributions from ^{13}C depleted periphyton to upstream DOC. However within-slump DOC is relatively more ^{14}C-enriched than within-slump POC (i.e. younger; figure 4(a)).

3.3. The effects of slumping on organic matter geochemical composition in streams (Goal 2)

Slumping effects on DOM and POM composition were most pronounced for POδ^{13}C and %POC. When compared to upstream values, within-slump runoff significantly differed in %POC, POδ^{13}C, POC:POP, DOC:DOP, and DOC:DON (table 2). Differences in POC:PN and Pδ^{15}N could not be tested statistically. However, POC:PN ratios upstream (11.4 ± 2.7, mean$\pm$ SD), within (11.6 ± 3.3), and downstream (10.8 ± 1.9) overlapped substantially (figure 3(k)), as did Pδ^{15}N values upstream (1.53 ± 0.89), within (1.48 ± 0.67), and downstream (1.60 ± 0.40). When comparing downstream to upstream locations, only %POC and POδ^{13}C were significantly different (table 2).

A principal components analysis of DOM and POM composition showed two major gradients (figure 5(a)). Only %POC, POC:POP, POC:PN, and POδ^{13}C variables had arrow lengths greater than the circle of equilibrium for the PCA analysis. Therefore these variables contributed the most to dispersion of sites in the reduced space and we focus on them for description of the gradients. PC1 (29%) clearly separated within-slump and downstream sites from upstream locations along a gradient that was indicative of variation in POM diagenetic state and periphytic contributions to POM, as indicated by %POC and POδ^{13}C. Along PC1, within-slump and downstream sites were more mineral- and ^{13}C-enriched relative to upstream sites, suggesting slump sediments had a greater proportion of degraded terrestrial material relative to fresher terrestrial material or in situ production (^{13}C depleted periphyton, figure 5(b)) characteristic of POC upstream (figure 4). No slump effect was apparent along PC2 (24%). Instead, PC2 reflected variation in POC: PN: POP stoichiometry. Runoff and upstream POM showed greater variability than downstream POM along this gradient, driven by nutrient-poor POM from active layer-dominated runoff (shallow slump SD) and an upstream site draining a catchment near the mountains (SE). This variation disappears for downstream samples, where POM is more universally nutrient enriched.

Incorporating headwall end-member sources into a PCA of POM geochemistry resulted in similar gradients of organic matter diagenesis/in situ contribution (along %POC and POδ^{13}C; PC1) and nutrient composition (POC:POP and POC:PN; figure 5(b), PC2). Organic matter from Holocene and Pleistocene permafrost was compositionally indistinguishable between horizons and from most within-slump samples. The upper active layer (O-horizon) had a greater organic carbon content (%POC) than permafrost and lower active layer samples, was more

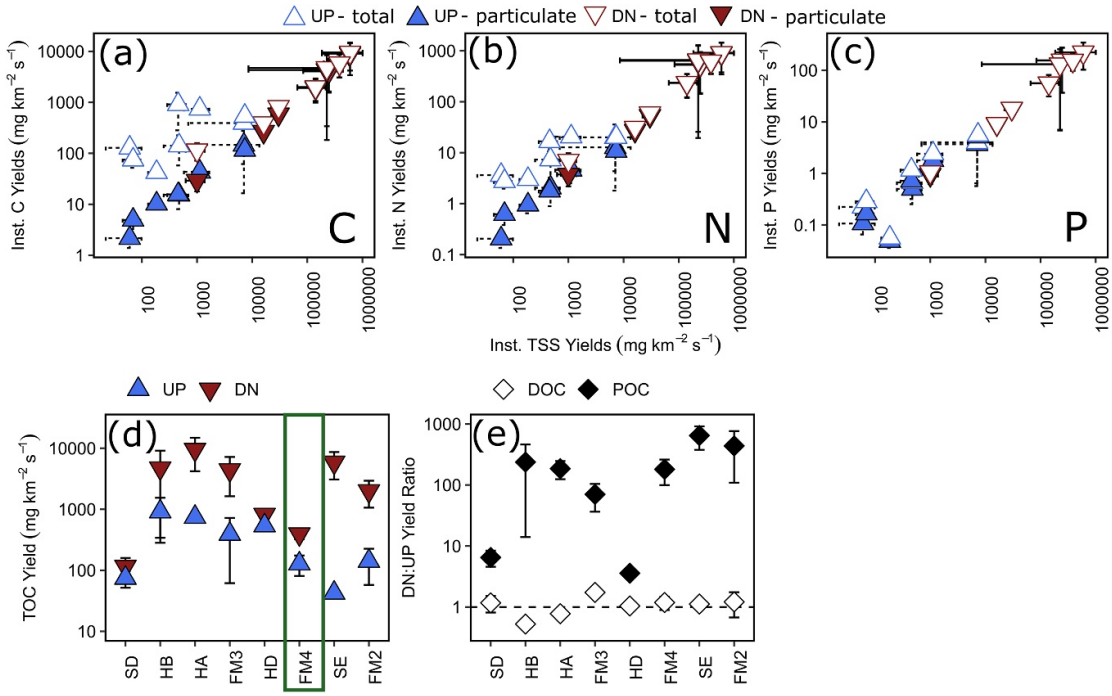

Figure 2. (a) Instantaneous carbon (C), (b) nitrogen (N), and (c) phosphorus (P) yields vs total suspended sediment (TSS) yields, upstream and downstream of thaw slumps. Filled triangles show particulate organic carbon (POC), particulate nitrogen (PN), and particulate organic phosphorus (POP) yields, while empty triangles show total organic carbon (TOC), total nitrogen (TN = total dissolved nitrogen + PN), and total phosphorus (TP = total dissolved phosphorus + POP) yields. (d) Suspended TOC yield upstream and downstream of thaw slump sites. (e) Downstream: upstream ratios (DN:UP) of particulate (POC) and dissolved (DOC) organic carbon yields. Whiskers represent standard error. There is only one HD upstream sample. The green box highlights slump FM4; most of the 'FM4′ headwall was not actively thawing during the sampling period. Slump sites on the x-axis are ordered left to right by increasing headwall height.

closely associated with upstream and within-slump runoff samples from SD (the shallowest slump), and was generally more nutrient depleted than permafrost sources. Both upper and lower active layer sources had greater variability in POC:PN and POC:POP than permafrost sources, which clustered at the more nutrient enriched end of PC2. Decreasing C:N ratios from upper active layer to permafrost has also been noted by Lacelle *et al* (2019) and is attributed to carbon mineralization, and thus degradation of organic matter since production.

3.4. The effects of slumping on the optical properties of based-extracted POM (Goal 2)

Five components were identified by PARAFAC (figures S1–2, table S1) (available online at stacks.iop.org/ERL/15/114019/mmedia), and matched components reported in other studies at Tucker congruences exceeding 0.95 (C1–C4) and 0.90 (C5) (www.openfluor.org; Murphy *et al* 2014). C1–4 were associated with terrestrial humic-/fulvic-like peaks, while C5 was associated with a tyrosine-/protein-like peak (table S1). Components 1–4 contributed upwards of 92% of F_{max} upstream, within-slump, and downstream of slumps, in agreement with findings of terrestrial organic matter dominance from mixing model results. C2 is similar to a component previously described as soil fulvic-like (table S1), and contributed similar proportions to F_{max} upstream (18% ± 2 se), within (20% ± 3 se), and downstream (19% ± 1 se) of slumps.

A PCA of BEPOM-derived optical characteristics revealed two clear gradients (figure 5(c)). The first was driven by contributions of C1, C3, and $a_{tot/TSS}$. Increasing $a_{tot/TSS}$ indicates greater chromophoric organic matter per unit sediment (i.e. Stubbins *et al* 2014), while C1 and C3 contrast two pools of terrestrial humic-like materials (see below). Along this gradient, within and downstream locations had greater values of %C1, but lower values of %C3 and $a_{tot/TSS}$ than upstream locations. We found a significant difference in %C1, the variable most strongly associated with this gradient, between stream locations (repeated measures ANOVA, $F_{2,4} = 8.34$, $p = 0.011$) due to differences between upstream %C1 (29 ± 3 se) vs. within (43 ± 3 se) and downstream (40 ± 3 se) locations (least-squared means; Lenth 2016). The second gradient in PCA space separated more biogeochemically-processed material (indicated by HIX, peak A:B and C:B; table S2) with greater molecular weight (S_R, Helms *et al* 2008) from 'fresh' or protein-like organic material (%C5). Across all sites, within-slump and downstream locations tended to be most closely associated with the more processed end of this gradient (figure 5(c)).

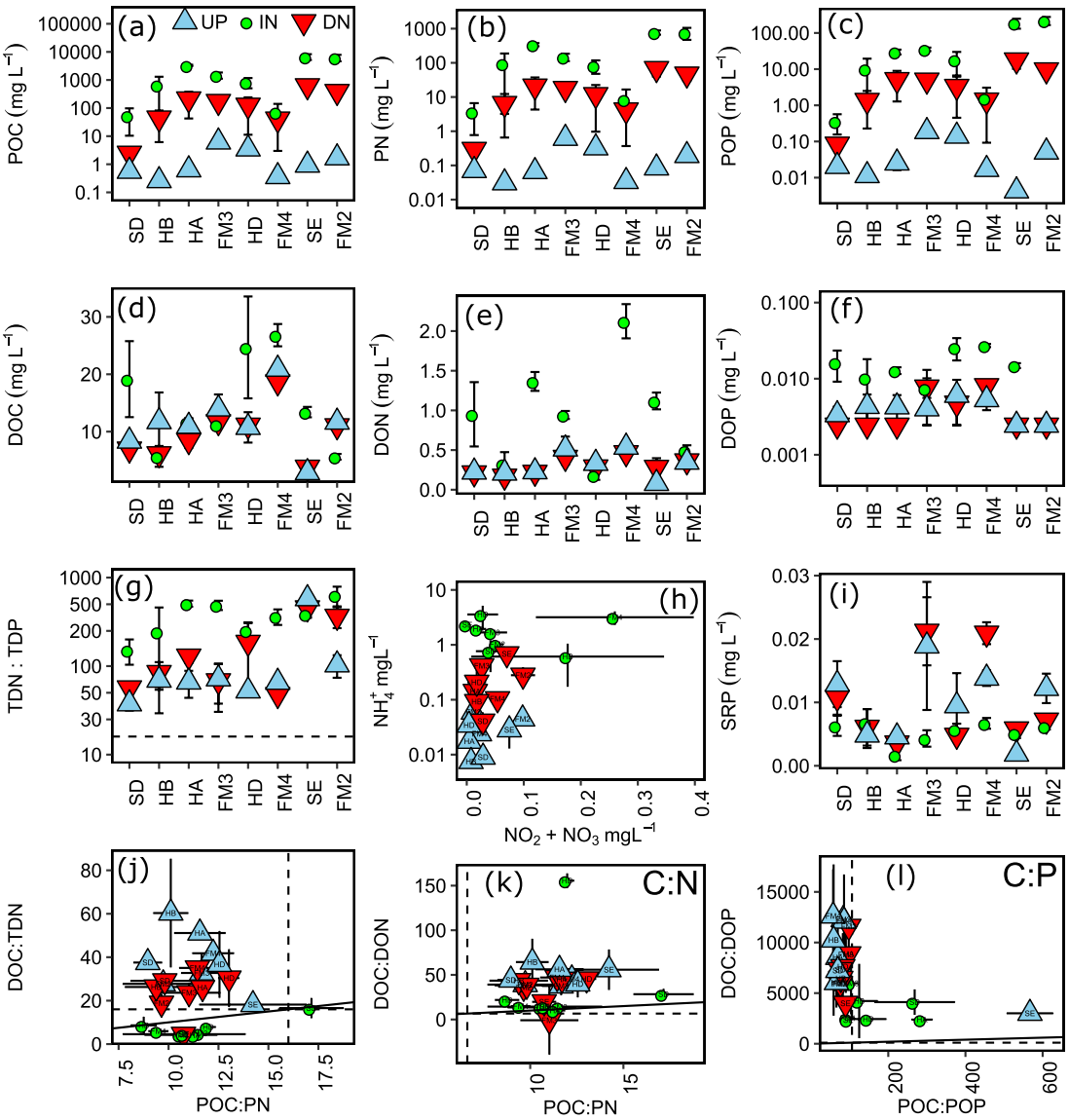

Figure 3. Upstream, within, and downstream comparisons of: (a-c) concentrations of particulate organic carbon (POC), particulate nitrogen (PN), and particulate organic phosphorus (POP); (d-f) concentrations of dissolved organic carbon (DOC), nitrogen (DON), and phosphorus (DOP); (g) total dissolved nitrogen vs. total dissolved phosphorus ratios (TDN:TDP); (h) NH_4^+ vs NO_2^- + NO_3^- concentrations; (i) soluble reactive phosphorus (SRP) concentrations; (j) organic carbon to total nitrogen atomic ratios in the dissolved and particulate phase; (k) DOM vs. POM C:N atomic ratios, assuming PN here accurately represents PON; (l) DOM vs POM C:P atomic ratios. Where, applicable, slump sites on the x-axis are ordered left to right by increasing headwall height. Dashed lines on ratio plots (j–l) demarcate Redfield ratios, a guideline which may indicate marine and freshwater nutrient limitation, while solid lines indicate the 1:1 ratio. Legend is in (a).

The %C1–%C3 gradient described above reinforces that slump sediments are more biogeochemically processed. C1 strongly resembles C1 of Stubbins *et al* (2014), which was identified as, 'an aggregation of highly diverse, relatively high molecular weight' terrigenous molecules that were 'carbon-rich and nitrogen poor'. In contrast, C3 resembles Stubbins-C3 and -C4 which both had greater nitrogen content, less conjugation or lower molecular weight, and greater homogeneity, suggesting these components have undergone less reworking since production. Thus, these results are consistent with inferences made from POM bulk geochemistry that within-slump and downstream material are relatively more degraded since production than upstream material (section 3.3).

3.5. The effects of morphological, meteorological, and landscape factors on slump-enabled changes in TOC yields and POM source and composition (Goal 3)

While TOC yields increased universally with slumping, this effect ranged from approximately two-fold to two orders of magnitude across sites (figure 2(a)) in association with headwall height ($\beta_{\text{std-height}} = 0.366 \pm 0.062$, $p = 0.004$), stream power ($\beta_{\text{std-spower}} = 0.251 \pm 0.055$, $p = 0.011$), and increasing westward location on the Peel Plateau

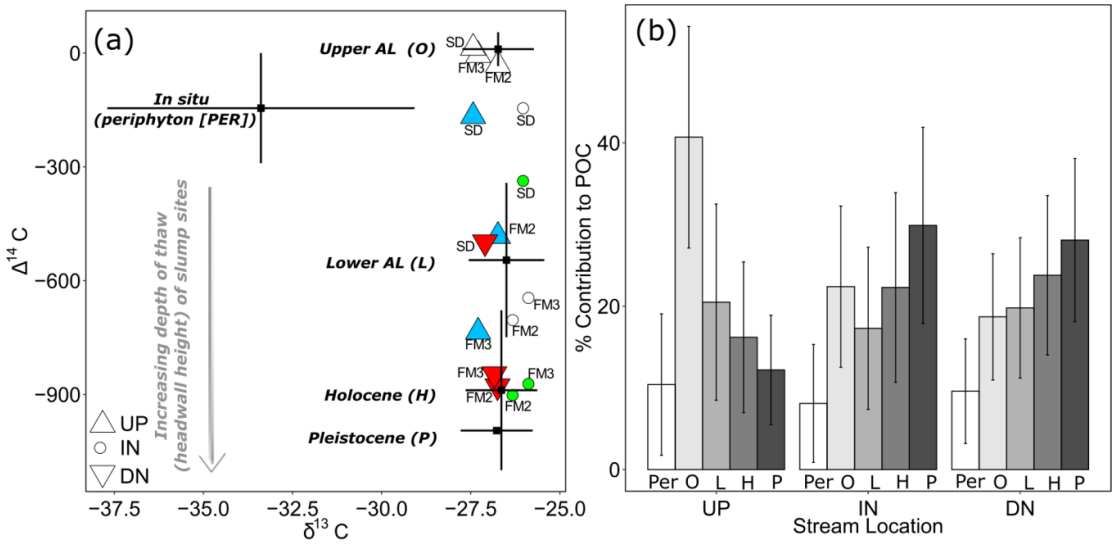

Figure 4. (a) Isospace plot of $\delta^{13}C$ vs. $\Delta^{14}C$ (‰) of POC sources and stream samples upstream, within, and downstream of select slump sites. Means ± 1 standard deviation of potential headwall [including Upper (O) and Lower (L) Active Layer, Holocene permafrost (H), and Pleistocene permafrost (P)] and in situ production [periphyton (PER)] sources are plotted (further details in supplementary S7). PO$\delta^{13}C$ standard deviations include ± 1‰ discrimination factor allowed in mixing model. Estimates of DO$\delta^{13}C$ and DO$\Delta^{14}C$ are shown via hollowed shapes using seasonal average values obtained from Zolkos and Tank (2019) and Littlefair *et al* (2017) respectively. (b) Mean and standard error of % contributions of sources in (a) upstream, within, and downstream locations for FM2, FM3, and SD.

($\beta_{std\text{-}long.} = -0.203 \pm 0.062$, $p = 0.031$). Headwall height ($\beta_{std\text{-}height} = 0.169 \pm 0.034$, $p = 0.007$, table 3) and longitude ($\beta_{std\text{-}long} = -0.154 \pm 0.031$, $p = 0.008$, table 3) were also significant predictors of differences in $(\%POC)^{-1}$ between upstream and within-slump locations. Upstream:within $(\%POC)^{-1}$ differences increased with increasing headwall height and westward location. In contrast, upstream: downstream variation in %POC was not explained by landscape or slump-associated variables, likely because %POC was less variable across downstream sites (figure 5).

Contributions of permafrost-origin materials to within-slump and downstream POM increased with headwall height (figure 4(a), table S5). Holocene- and Pleistocene-age permafrost contributions to downstream POC increased from 18.5 ± 18.5% and 14.4 ± 15%, respectively (mean ± se) at SD (~ 2 m max. height, table 1) to 31.5 ± 34.4% and 50 ± 35.3% at FM3 (~10.3 m max. height) and 31.4 ± 32.1% and 49.6 ± 29.1% at FM2 (~25 m max. height). In particular, POC from Pleistocene-age permafrost doubled in contribution from SD to FM2. Within-slump POM molecular structure, inferred from BEPOM, also varied with headwall height, and this variation was similarly lost downstream. Within-slump BEPOM fluorescence ranged from being indistinguishable from upstream sites at the shallowest slump (SD), to being substantially enriched in %C1 at the largest features (FM2; table 1; figure 5(c)). This variation did not persist downstream as POM downstream of FM2 and SD became more similar to other slump sites.

4. Discussion

Slumping caused orders of magnitude increases in TOC and nutrient delivery to streams via the thaw-driven mobilization of sediments. This mobilization was dominantly in the form of POC, PN, and POP, shifting streams from dissolved to particulate dominated systems. Slumping increased permafrost organic carbon in stream networks, however within-slump POC values were more ^{14}C-depleted (older) than values previously recorded for DO^{14}C (figure 4(a), Littlefair *et al* 2017) indicating POC mobilizes a greater degree of aged organic matter from deeper permafrost deposits. Optical properties of base-extracted POM indicated slump-mobilized POM was more processed since production than material present upstream.

Slumping increased TOC yields to a greater degree at sites with greater maximum headwall height and downstream stream power. Increasing thickness of permafrost thawed, associated with headwall height, may increase hydrologic input from melting of massive ice (Rudy *et al* 2017) which can increase sediment transport at baseflow (Kokelj *et al* 2013). Across the Peel Plateau, headwall heights and the depth of permafrost thawed generally increase as slumping intensifies and connects to streams, with slump-stream connectivity typically occurring at maximum headwall heights greater than ~2 m (Kokelj et al under review). Thus, as slumping intensifies, stream TOC yields may increase due to increased delivery of POC. However this increase will also depend on the stream's transportation potential (i.e. stream power), which

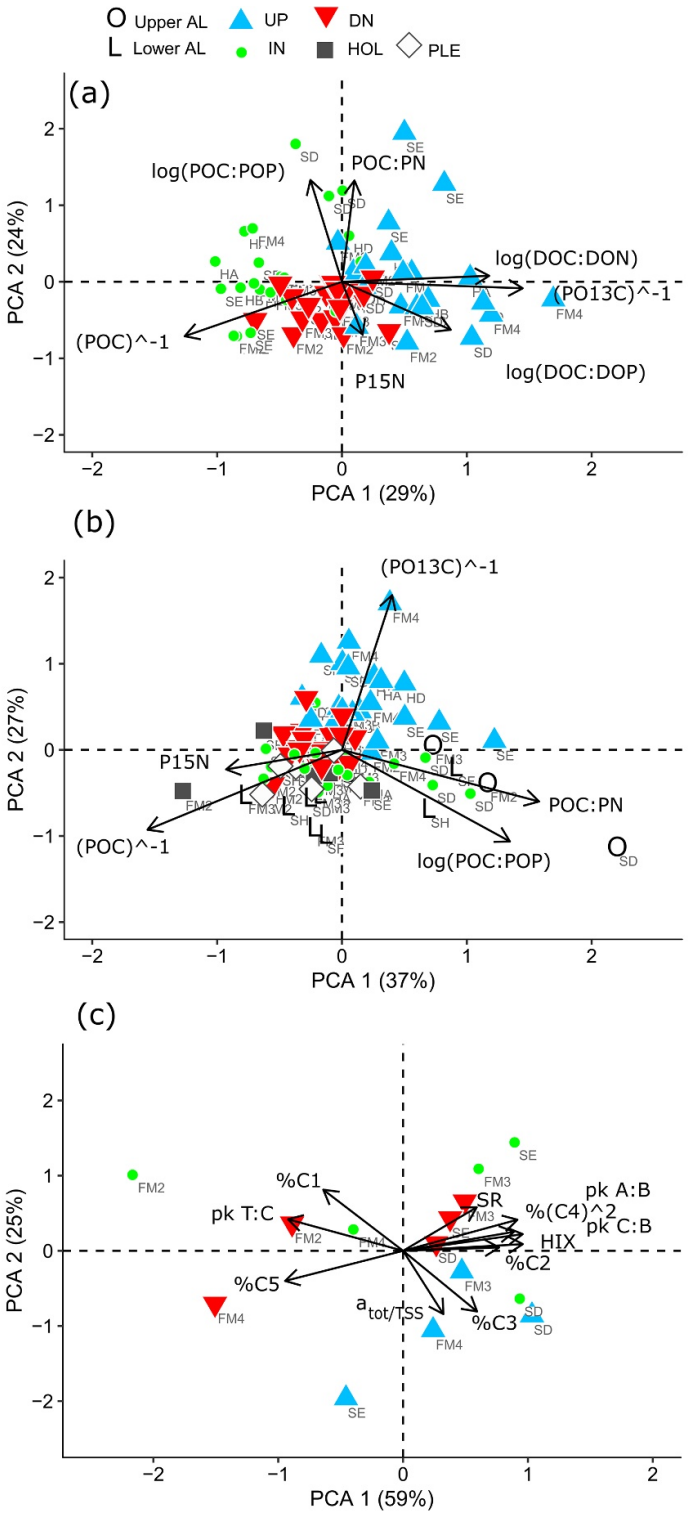

Figure 5. PCA results for: (a) Geochemical composition of suspended particulate organic matter (POM) and dissolved organic matter (DOM) in runoff and stream water. (b) Geochemical composition of suspended POM in stream water, and values from stratigraphic samples for slump headwalls [Upper (O) and Lower (L) Active Layer, Holocene permafrost (HOL), and Pleistocene permafrost (PLE) are shown]. (c) Base extracted POM [BEPOM] fluorescent components (%C1-5) and optical indices (see table S2).

we discuss further in section 4.2. Landscape position also played an important role as TOC yields increased to a greater degree westwards on the Peel Plateau, with closer proximity to late-glacial limits, where elevation and relative relief is greater, tundra vegetation is sparser, and fine-grained tills, with a greater abundance of glaciofluvial/glaciolacustrine deposits, are veneered over bedrock (Duk-Rodkin and Hughes 1992). Since maximum scar-valley slope was not a significant predictor of TOC yields, the combination of sparse vegetation and fine-grained, ice-rich deposits veneering bedrock appear to make the terrain near

Table 3. Effects of morphological, landscape, and stream power variables on variation in log(TOC yield) and (%POC^{-1}) across slump sites. Only explanatory variables retained in final models are shown. Estimates are standardized. Starting variables for all models consisted of maximum headwall height, debris tongue length, total rainfall over the past 96 h, longitude of the slump site, and downstream stream power (except for the upstream: within model). Maximum slope was also used for the TOC yield model.

Variable (scaled and centered)	Estimate	Error	t	P
upstream: downstream log (TOC yield)	($R^2_{adj.} = 0.8677$)			
Max. Headwall Height (m)	0.366	0.062	5.914	**0.004**
Downstream stream power	0.251	0.055	4.530	**0.011**
Longitude	−0.203	0.062	−3.265	**0.031**
Intercept	0.000	0.051	0.000	1.000
upstream: within (%POC^{-1}) [a]	($R^2_{adj.} = 0.8112$)			
Max. Headwall Height (m)	0.169	0.034	5.031	**0.007**
Longitude	−0.154	0.031	−4.951	**0.008**
Total Rainfall (mm, past 96 h) [b]	0.040	0.030	1.330	0.254
Intercept	0.000	0.026	0.000	1.000
upstream: downstream (%POC^{-1})				
No explanatory variables found to be significant				

[a]stream power was not entered as a variable in the starting model
[b]retained to improve model residuals

the western margin of the glacial limit particularly susceptible to thaw-driven erosion. Headwall height and landscape position also affected the organic carbon content of within-slump particles and divergence from upstream particles, with headwall height also increasing the proportion of more decayed organic matter of within-slump POM (section 3.5). However, we found no significant predictors of differences in composition between upstream and downstream %POC, and site variation in upstream-to-within BEPOM differences decreased downstream of thaw slumps, despite the fact that Holocene- and Pleistocene-age permafrost contributions to downstream POC were greater at sites with greater headwall heights. We discuss this further in section 4.3. Finally, though our study focused on actively eroding slumps, slump stabilization, which can occur if collapsed debris accumulates at the base of the headwall and insulates exposed ice (Kokelj *et al* 2015), was evident at FM4 where most of the headwall was not actively eroding during our sampling period. This may be why TOC concentrations did not increase substantially and within-slump POC, PN, and POP concentrations are more similar to SD, the smallest slump in this study. Notably, POC yields still increased downstream of slump FM4, likely due to stream erosion of the ~1 km debris tongue.

4.1. Significance of thermokarst-derived POC and implications for permafrost-carbon release and fate

Particulate dominance of organic carbon mobilization is likely common in hillslope thermokarst systems throughout the circumpolar Arctic, based on previous records of high POC and sediment concentrations within or downstream of thermokarst features in Siberia (Vonk *et al* 2013), the Eastern Canadian high Arctic (Lamoureux and Lafrenière 2014, Beel *et al* 2020), and Alaska (Bowden *et al* 2008). Furthermore, the Peel Plateau shares similarities to permafrost preserved glaciated landscapes observed to contain thaw slumps in Alaska and Siberia (Kokelj *et al* 2017a). Yet studies assessing controls on mobilization (Bröder *et al* 2020, Tanski *et al* 2017) and mineralization (Attermeyer *et al* 2018, Tanski *et al* 2019) of permafrost-origin POC are sparse, particularly in comparison to DOC, despite particles being noted as important sites for carbon mineralization in streams (Attermeyer *et al* 2018), or, conversely, agents of carbon sequestration (Hemingway *et al* 2019).

On the Peel Plateau, slump-mobilized POC appears to be at a greater stage of decay than relatively more modern material present upstream, as inferred from depleted organic carbon content, and relative increase in a fluorescent component (C1) that has been described as a diverse array of relatively high molecular weight molecules (Stubbins *et al* 2014). This suggests reduced bioavailability of stream POC. This is in agreement with Lacelle *et al* (2019) where ^{13}C NMR analysis of slump headwalls has shown that active layers contain young and more biodegradable forms of organic carbon (O-alkyl-C and narrow Alkyl-C), while undisturbed permafrost and relict-thaw layers, if not comprised of colluvium from past slumping , contain older and relatively more recalcitrant aromatic compounds. Calibrated dates of Pleistocene-age permafrost in this study are > 40 000 yrs B.P. (table S4), in agreement with previous work that suggests a significant amount of soil organic carbon within Pleistocene-age permafrost likely originates from regional vegetation growing prior to the advance of the LIS (Lacelle *et al* 2019). However, shale bedrock, including black shales with > 2 wt% TOC (Allen *et al* 2015), was likely also eroded and entrained in glacial till (Norris 1985, Calmels *et al* 2007). Thus petrogenic organic carbon, which is 'radiocarbon

dead', cannot be excluded as another important component of material preserved within Pleistocene-age deposits.

Our findings of relatively more decayed slump-mobilized POC broadens previous findings that slump-derived DOC on the Peel Plateau has reduced aromaticity and molecular weight, and elevated biolability compared to that from unimpacted streams (Littlefair *et al* 2017, Littlefair and Tank 2018). This suggests that DOM and POM pools are compositionally distinct and slumping affects the two pools in contrasting ways. Compositional differences could be due in part to different source contributions to the POC vs. DOC pools. $\Delta^{14}C$ values suggest that organic carbon from Pleistocene-age permafrost contributes proportionately less to DOC than POC, which is further supported by ground ice measurements on the Peel Plateau that show that DOC concentrations are greater in Holocene-age permafrost (15.36 $\pm$ 14.16 mg l^{-1}; Zolkos and Tank 2019) than Pleistocene-age permafrost (2.58 $\pm$ 2.19 mg l^{-1}; mean $\pm$ SD, n = 8). Furthermore, DOM stoichiometry is starkly different from POM stoichiometry, the latter of which closely resembles Holocene and Pleistocene headwall organic matter stoichiometry. This difference could be due to ongoing processing of DOM in permafrost porewaters (Ewing *et al* 2015) and partial sorption/desorption that preferentially enables aliphatic moieties to remain dissolved (Littlefair and Tank 2018). These findings are corroborated by work on Herschel Island, an ice marginal feature along the Yukon north coast, where the degradation of permafrost material exposed in slump headwalls was largely driven by degradation in the dissolved phase (Tanski *et al* 2019). Given that tills on Herschel Island contain a greater proportion of marine sediments, and thus likely differ somewhat in their composition to those from the Peel Plateau (Kokelj *et al* 2002, Lane *et al* 2012, Tanski *et al* 2017), this result suggests that our findings may be relevant across the broader glacial margin region of the western Canadian Arctic.

In terms of the broader Arctic, our finding of more decayed slump-mobilized POC does contrast with recent findings that permafrost-influenced POM in the Kolyma River is less degraded than that derived from a headwater stream primarily influenced by in-stream production and recent vegetation, as assessed by lipid degradation proxies (Bröder *et al* 2020). This difference may be due to differences in the sources and genesis of permafrost between the two regions. While permafrost on the Peel Plateauwas formed following the deposition of glacial tills within which petrogenic organic carbon is likely an important component (see below), permafrost thaw in the Kolyma River region unearths deposits in the Yedoma domain, formed from the simultaneous accumulation of ground ice and sediment/organic matter deposition (syngenetic) in non-glaciated regions typically with low topographic relief (Schirrmeister *et al* 2013, Strauss *et al* 2017). Contrasts in geological origins of these two permafrost environments may also influence the nature of material mobilization. The remobilization of sediments and organic carbon to fluvial networks in the Yedoma domain tends to be documented along larger rivers and coastlines, while direct impacts to fluvial networks on the Peel Plateaupredominantly occur in headwater streams where fluvial incision has engendered high topographic relief (Tank *et al* 2020, Kokelj et al under review). Thus we need more studies examining/including thermokarst-POC mobilization in different landscapes to understand its release and fate in relation to landscape state factors (Tank et al 2020).

Petrogenic organic carbon, likely an important component of Pleistocene-origin POC in this study, is generally considered resistant to remineralization (Blattmann *et al* 2018). However, the balance between oxidation of petrogenic organic carbon, a source of CO_2 (Horan *et al* 2019) and burial of biospheric organic carbon, a sink of CO_2 (Hilton *et al* 2015) plays an important role in determining the status of the Mackenzie River basin as a net source or sink to the atmosphere (Horan *et al* 2019). Thus enhanced erosion of organic carbon via thaw slumps on the Peel Plateau highlights the importance of asessing the reactivity of slump-mobilized POC and emphasizes the growing recognition of fluvial networks as important components of carbon cycling in northern ecosystems (Plaza *et al* 2019), particularly in thermokarst terrains (Turetsky *et al* 2020).

4.2. Implications of sediment transport limitation for permafrost-carbon fate

Our study focuses on suspended particles, yet the majority of terrestrial material eroded via slumping accumulates within valley-bottom debris tongues (Kokelj *et al* under review, Kokelj *et al* 2015, van der Sluijs *et al* 2018). Fluvial erosion of these deposits are limited by the stream's transport capacity as illustrated by the significant role stream power plays in explaining suspended TOC yield variations in this study. At FM2 and FM3, ~ 30% of the terrestrial volume excavated by slumping is contained within slump debris tongues (Kokelj *et al* under review, van der Sluijs *et al* 2018). When accounting for the fact that the upper 10 m of permafrost can contain greater than 50% ground ice content (Malone *et al* 2013, Lacelle *et al* 2015), the debris tongue likely contains greater than 80% of the soils and sediments evacuated by slumping, since melted ground ice is lost via runoff and evaporation. Debris tongues at FM3 and the immediately downstream FM2 have estimated volumes of 19.5 and 1.5 10^5 m^3 (van der Sluijs *et al* 2018, Kokelj *et al* under review). If we assume a single density of sediments (2.65 g cm^{-3}; Armanini *et*

al 2018) and estimate 2% of sediment is POC (using suspended sediment %POC data from FM2-DN and FM3-DN in this study), this 15.95 km^2 catchment contains ~ 1.1×10^{11} g slump-origin POC in debris tongue deposits. We estimate that POC may remain within these primary sediment stores (Murton and Ballantyne 2017) for hundreds (~1.4×10^2) to thousands (~1.1×10^3) of years. This estimate is based on scaling of average downstream suspended POC fluxes (FM2-DN, this study) through the active thaw season (April 30th to September 30th inclusive, 154 d, O'Neill *et al* 2015), with an error range of −75% to + 100%. Our error range is roughly based on differences noted between scaling average SD fluxes vs calculations with turbidity calibrated by TSS flux and %POC data (supplementary S10) and uncertainty in the duration of active stream erosion throughout the year. This storage estimate does not take stream beload transport into account, and we recommend future studies include measurements of bedload transport to increase accuracy of storage estimates.

The intensification of thaw slump activity and disturbance enlargement is causing a rapid, net accumulation of materials in valley bottom debris tongue deposits (van der Sluijs *et al* 2018, Kokelj *et al* under review). Though not located in the valley bottom, preserved organic matter within colluvial deposits of headwalls suggests that the accumulation of thawed material may inhibit organic matter decomposition (Lacelle *et al* 2019, Zolkos and Tank 2020). POC that is transported away from the thaw site by the stream will also fluctuate between deposition and transport, dependent on particle density and size. When settled out, mineralization of organic carbon can be reduced ~50% (Richardson *et al* 2013) or more, particularly if contained in anoxic sediments (Peter *et al* 2016), though DOC can diffuse from sediments to be mineralized in oxic waters (Peter *et al* 2016). Across the western Canadian Arctic, the volume of terrestrial material excavated from landscapes by slumping is accelerating (Kokelj *et al* 2015, Kokelj *et al* under review, Lewkowicz and Way 2019), with slumping primarily occurring on low order streams with less power for sediment transportation than the larger Peel and Mackenzie rivers (Kokelj *et al* 2017a, Kokelj *et al* under review). This suggests that hillslope thermokarst models, where the majority of carbon is laterally exported and a substantial proportion is assumed to be mineralized (e.g. one-third, Turetsky *et al* 2020), may overestimate carbon mineralization. Improved prediction of the fate of permafrost carbon released by slope thermokarst requires that sediment cascade frameworks, and assessments of organic carbon reactivity within that framework, be integrated into modelling efforts.

4.3. Ecological implications for stream systems

Increasing sediment mobilization due to thermokarst activity can directly decrease foodweb production by decreasing stream benthic invertebrate abundance (Chin *et al* 2016), and by shifting food webs to become more reliant on decomposition of terrestrial organic carbon than in-stream primary production, as a result of the negative effects of sediments on autochonous production (Levenstein *et al* 2018). Thus, the composition of terrestrial inputs may play an important role in changes in stream ecological function and the basal energy resources that support higher trophic level production.

Differential organic matter composition is a well-established driver of variation of microbial metabolism (Sinsabaugh and Follstad Shah 2012, Ward and Cory 2015, Roiha *et al* 2016, Panneer Selvam *et al* 2017, Jain *et al* 2019). Thus, the divergent composition of permafrost-origin DOM and POM in this study suggests that DOM-based assessments of microbial production and mineralization rates are unlikely to be accurate for POM. In our study, the low POC:POP ratios relative to DOC:DOP, are closer to mean C:P values of aquatic microbial biomass obtained from the literature (166 with approximately three-fold variation; Sinsabaugh *et al* 2013), suggesting that microbial biomass production could be greater on POM than estimates based solely on DOM, if organisms are P-limited and if the lower C:P ratios in POM is not solely due to living microbial biomass (Sinsabaugh and Follstad Shah 2010, Franklin *et al* 2011). TDN:TDP ratios were typically more than double Redfield ratios and, in some cases, increased downstream due to high TDN:TDP within slump ratios, suggesting limited phosphorus supply in the dissolved phase and that POM could be an important source of phosphorus to microbes. Yet the diagenetic state of POM in this study suggests low lability, thus low C:N and C:P ratios may be due to incorporation of N and P in humic complexes (Grandy and Neff 2008, Sinsabaugh and Follstad Shah 2011). In addition, some particulate nitrogen may be inorganic nitrogen sorped to clay structures (Schubert and Calvert 2001). Complexation in combination with non-competitive sorption of enzymes to mineral and organic colloids in particle-rich environments, may decrease metabolic efficiency (Schimel and Weintraub 2003, Grandy and Neff 2008) and microbial growth rates (Moorhead and Sinsabaugh 2006). This highlights the need to include particle-associated microbial communities and enzymes in assessments of rates of microbial production and mineralization (Sinsabaugh and Shah 2012) to understand how the abrupt shift in the quantity and

composition of organic matter delivered to streams may affect resource flow through stream food webs (Sinsabaugh and Shah 2013), and thus stream ecological function and it is role in regional or global biogeochemical cycles.

Despite differences in within-slump POM, consistent convergence of downstream POM composition suggests that slump-POM material is well mixed prior to entry into modern stream networks. Headwall ablation, accumulation of a saturated slurry of thawed materials, and downslope sediment transport by surface flow and deeper seated flow contributes significantly to physical mixing of slumped materials (Kokelj *et al* 2015, van der Sluijs 2018) that were previously distinguishable in stratigraphy. Furthermore, biochemical processing within the slump scar zone (Abbott *et al* 2015, Tanski *et al* 2017) may be enhanced by the warm and wet conditions that distinguish this environment (Kokelj *et al* 2009, van der Sluijs *et al* 2018). This suggests that compositional differences between slumps may be less important than the quantity of POM for driving differences in downstream microbial processing between slump sites and/or that the initial unimpacted stream system state is important in understanding the effect of slumping on change to a stream system since upstream locations in this study had greater variation than downstream locations. Further long-term studies of changing biogeochemical function as slumps undergo variations in headwall erosion rates would help assess this. Of course, this interpretation is limited by the sensitivity of our analyses. Further work detailing specific organic compounds (e.g. via solid-state NMR, Mccallister *et al* 2018; or Pyrolysis-Gas Chromatography-Mass Spectrometry, Py-GC/MS; Ma *et al* 2018) is required. In addition, the shift of streams from DOC to POC dominated systems highlights the need to use tools that can be applied to both dissolved and particulate phases of organic matter and associated microbial activity.

Finally, slump-associated particle release along fluvial networks creates potential for ecological and biogeochemical effects to be carried far from the site of thaw. The headwaters of the Peel Plateau drain into the Peel River, which has an annual sediment flux greater than most major Russian-Arctic Rivers (Holmes *et al* 2002). Currently, the contribution of thermokarst-derived sediments and POC to this flux is an important unknown. Using turbidity data and relationships between turbidity and TSS, POC, PN, and POP (supplementary S10) we estimate that POC, PN, and POP yields downstream of the smallest slump in this study (SD) are approximately 3.0×10^5, 3.9×10^4, and 1.0×10^4 kg km^{-2} from mid-June to mid-August (supplementary S10, figure S7). These estimated yields are orders of magnitude greater than the combined dissolved and particulate carbon and nitrogen yields of any of the major Arctic rivers, including the Mackenzie River (Mcclelland *et al* 2016). Thaw slumping along these headwaters is thus likely to increase downstream nutrient and organic carbon subsidies and act as a hotspot for nutrient and organic matter transfer from land to fluvial networks. Though the majority of material excavated from thaw slumps is being temporarily contained within debris tongue deposits, these primary sediment stores are readily available for stream transport, and will cascade through a sequence of storage reservoirs through downstream systems over the coming millennia (Kokelj et al under review). This also highlights, as previously noted (Kokelj *et al* 2015, Beel *et al* 2018), that hydrometeorological change will play an important role in propagation of effects to downstream systems.

5. Conclusions

In permafrost regions where slope thermokarst is a dominant mechanism of thaw-driven change, we show that the vast majority of organic carbon mobilization to stream networks occurs via POC. Particulate organic matter mobilized from thaw slumps, and associated POC, is compositionally distinct from the dissolved phase, in part due to the range of distinct material types that have been preserved by permafrost. This will likely translate into differences in carbon mineralization rates and roles in nutrient cycling between the two phases. Estimated yields from slumps suggest that these features create a hotspot for particulate C, N, and P release to fluvial networks. While the majority of material mobilized by thaw slumping is deposited in valley-bottom stores, these massive repositories of readily-mobilized material can switch streams from dissolved- to particulate-dominated systems and will create a step change in the ecological and biogeochemical functioning of downstream systems that is irreversable over century to millenial timescales. The dominance of sediment-associated C, N, and P release from thaw slumps highlights the pressing need for better knowledge of sedimentary cascades, mobilization, and storage reservoirs in slump-affected streams, and baseline assessments of the microbial processing of POM and cycling of particulate nutrients within a sedimentary cascade framework.

Data availability statement

The data that support the findings of this study are openly available at the following URL/DOI: https://doi.org/10.21963/13160.

Acknowledgments

We are thankful for support from the Tetlit Gwich'in Renewable Resources Council and Aurora Research Institute, and field assistance of Joyce Kendon, Luke Gjini, Maya Guttman, Lindsay Stephens, Christine

Firth, Elizabeth Jerome, Billy Wilson, Keith Colin, Rosemin Nathoo, and Erin MacDonald. Cara Littlefair provided invaluable advice on field logistics, and was involved in initial site selection of HA, HB, HD, and SD. Shawne Kokelj provided meteorological data. Alberto Reyes provided advice on headwall source sampling. Christopher Osburn advised laboratory BEPOM analyses and he and Ashley Dubnick provided advice on PARAFAC modelling. Christine Ridenour assisted with BEPOM analyses. Casey Beel provided advice on interpretation of turbidity sensor data. Research was financially supported by the Aurora Research Fellowship, Garfield Weston Foundation, Northern Scientific Training Program, UAlberta North, Natural Sciences and Engineering Research Council of Canada, Environment Canada Science Youth Horizons Program, Arctic Institute of North America, and Polar Continental Shelf Program. Northwest Territories Geological Survey (NTGS) contribution #0128. Finally, thank you to two anonoymous reviewers whose comments improved this manuscript.

ORCID iDs

S Shakil https://orcid.org/0000-0002-8877-4830
S E Tank https://orcid.org/0000-0002-5371-6577
J E Vonk https://orcid.org/0000-0002-1206-5878
S Zolkos https://orcid.org/0000-0001-9945-6945

References

Abbott B W, Larouche J R, Jones J B, Bowden W B and Balser A W 2014 Elevated dissolved organic carbon biodegradability from thawing and collapsing permafrost *J. Geophys. Res. Biogeosci.* **119** 2049–63

Abbott B W, Jones J B, Godsey S E, Larouche J R and Bowden W B 2015 Patterns and persistence of hydrologic carbon and nutrient export from collapsing upland permafrost *Biogeosciences* **12** 3725–40

Allen T L, Fraser T A, Hutchinson M P, Dolby G, Reyes J and Utting J 2015 OF2015-3.pdf (Yukon geological survey) Online: http://ygsftp.gov.yk.ca/publications/openfile/2015/OF2015-3.pdf

Armanini A 2018 *Introduction to Sediment Transport Principles of River Hydraulics* (Berlin: Springer) 33–47

Attermeyer K, Catalán N, Einarsdottir K, Freixa A, Groeneveld M, Hawkes J A, Bergquist J and Tranvik L J 2018 Organic carbon processing during transport through boreal inland waters: particles as important sites *J. Geophys. Res.* **123** 2412–28

Bates D, Mächler M, Bolker B and Walker S 2015 Fitting linear mixed-effects models using lme4 *J. Stat. Softw.* **67** 1–48

Beel C R, Lamoureux S F and Orwin J F 2018 Fluvial response to a period of hydrometeorological change and landscape disturbance in the Canadian High Arctic *Geophys. Res. Lett.* **45** 446–10

Beel C R, Lamoureux S F, Orwin J F, Pope M A, Lafrenière M J and Scott N A 2020 Differential impact of thermal and physical permafrost disturbances on High Arctic dissolved and particulate fluvial fluxes *Sci. Rep.* **10** 11836

Blattmann T M, Letsch D and Eglinton T I 2018 On the geological and scientific legacy of petrogenic organic carbon *Am. J. Sci.* **318** 861–81

Bowden W B, Gooseff M N, Balser A, Green A, Peterson B J and Bradford J 2008 Sediment and nutrient delivery from thermokarst features in the foothills of the North Slope, Alaska: potential impacts on headwater stream ecosystems *J. Geophys. Res.* **113** n/a-n/a

Brett M T *et al* 2017 How important are terrestrial organic carbon inputs for secondary production in freshwater ecosystems? *Freshw. Biol.* **62** 833–53

Brooker A, Fraser R H, Olthof I, Kokelj S V and Lacelle D 2014 Mapping the activity and evolution of retrogressive thaw slumps by tasselled cap trend analysis of a landsat satellite image stack *Permafrost Periglacial Process.* **25** 243–56

Brym A, Paerl H W, Montgomery M T, Handsel L T, Ziervogel K and Osburn C L 2014 Optical and chemical characterization of base-extracted particulate organic matter in coastal marine environments *Mar. Chem.* **162** 96–113

Bröder L, Davydova A, Davydov S, Zimov N, Haghipour N, Eglinton T I and Vonk J E 2020 Particulate organic matter dynamics in a permafrost headwater stream and the Kolyma River mainstem *J. Geophys. Res.* e2019JG005511

Burd K, Estop-Aragonés C, Tank S E and Olefeldt D 2020 Lability of dissolved organic carbon from boreal peatlands: interactions between permafrost thaw, wildfire, and season *Can. J. Soil. Sci.* 1–13

Burn C R 1997 Cryostratigraphy, paleogeography, and climate change during the early Holocene warm interval, western Arctic coast, Canada *Can. J. Earth Sci.* **34** 912–25

Calmels D, Gaillardet J, Brenot A and France-Lanord C 2007 Sustained sulfide oxidation by physical erosion processes in the Mackenzie River basin: climatic perspectives *Geology* **35** 1003

Chin K S, Lento J, Culp J M, Lacelle D and Kokelj S V 2016 Permafrost thaw and intense thermokarst activity decreases abundance of stream benthic macroinvertebrates *Glob. Change Biol.* **22** 2715–28

Duk-Rodkin A and Hughes O L 1992 (Geological Survey of Canada) Ottawa A Series Map 1745A 1:250,000

Dyke A 2005 Late quaternary vegetation history of Northern North America based on Pollen, Macrofossil, and Faunal remains *Géogr. Phys. Quat.* **59** 211–62

Ewing S A, O'Donnell J A, Aiken G R, Butler K, Butman D, Windham-Myers L and Kanevskiy M Z 2015 Long-term anoxia and release of ancient, labile carbon upon thaw of Pleistocene permafrost *Geophys. Res. Lett.* **42** 730–10

Finlay J C and Kendall C 2008 Stable isotope tracing of temporal and spatial variability in organic matter sources to freshwater ecosystems *Stable Isotopes in Ecology and Environmental Science* (New York: Wiley) pp 283–333

Franklin O, Hall E K, Kaiser C, Battin T J and Richter A 2011 Optimization of biomass composition explains microbial growth-stoichiometry relationships *Am. Nat.* **177** E29–42

Fuchs M, Grosse G, Strauss J, Günther F, Grigoriev M, Maximov G M and Hugelius G 2018 Carbon and nitrogen pools in thermokarst-affected permafrost landscapes in Arctic Siberia *Biogeosciences* **15** 953–71

Fuchs M, Lenz J, Jock S, Nitze I, Jones B M, Strauss J, Günther F and Grosse G 2019 Organic carbon and nitrogen stocks along a thermokarst lake sequence in Arctic Alaska *J. Geophys. Res.* **124** 1230–47

Grandy A S and Neff J C 2008 Molecular C dynamics downstream: the biochemical decomposition sequence and its impact on soil organic matter structure and function *Sci. Total Environ.* **404** 297–307

Gundelwein A, Müller-Lupp T, Sommerkorn M, Haupt E T K, Pfeiffer E-M and Wiechmann H 2007 Carbon in tundra soils in the Lake Labaz region of arctic Siberia *Eur. J. Soil Sci.* **58** 1164–74

Guo F, Kainz M J, Sheldon F and Bunn S E 2016 The importance of high-quality algal food sources in stream food webs – current status and future perspectives *Freshw. Biol.* **61** 815–31

Guo L and Macdonald R W 2006 Source and transport of terrigenous organic matter in the upper Yukon River: evidence from isotope (δ13C, Δ14C, and δ15N)

composition of dissolved, colloidal, and particulate phases *Glob. Biogeochem. Cycles* **20** GB2011
Guo L, Ping C-L and Macdonald R W 2007 Mobilization pathways of organic carbon from permafrost to arctic rivers in a changing climate *Geophys. Res. Lett.* **34** L13603
Helms J R, Stubbins A, Ritchie J D, Minor E C, Kieber D J and Mopper K 2008 Absorption spectral slopes and slope ratios as indicators of molecular weight, source, and photobleaching of chromophoric dissolved organic matter *Limnol. Oceanogr.* **53** 955–69
Hemingway J D, Rothman D H, Grant K E, Rosengard S Z, Eglinton T I, Derry L A and Galy V V 2019 Mineral protection regulates long-term global preservation of natural organic carbon *Nature* **570** 228–31
Hilton R G, Galy V, Gaillardet J, Dellinger M, Bryant C, O'Regan M, Gröcke D R, Coxall H, Bouchez J and Calmels D 2015 Erosion of organic carbon in the Arctic as a geological carbon dioxide sink *Nature* **524** 84–87
Holmes R M, Mcclelland J W, Peterson B J, Shiklomanov I A, Shiklomanov A I, Zhulidov A V, Gordeev V V and Bobrovitskaya N N 2002 A circumpolar perspective on fluvial sediment flux to the Arctic ocean *Glob. Biogeochem. Cycles* **16** 45–1
Horan K *et al* 2019 Carbon dioxide emissions by rock organic carbon oxidation and the net geochemical carbon budget of the Mackenzie River Basin *Am. J. Sci.* **319** 473–99
Jain A, Krishnan K P, Singh A, Thomas F A, Begum N, Tiwari M, Bhaskar V P and Gopinath A 2019 Biochemical composition of particles shape particle-attached bacterial community structure in a high Arctic fjord *Ecol. Ind.* **102** 581–92
Kokelj S V and Jorgenson M T 2013 Advances in thermokarst research *Permafrost Periglacial Process.* **24** 108–19
Kokelj S V, Kokoszka J, van der Sluijs J, Rudy A C A, Tunnicliffe J, Shakil S, Tank S and Zolkos S Under Review Permafrost thaw couples slopes with downstream systems and effects propagate through Arctic drainage networks The Cryosphere (https://doi.org/10.5194/tc-2020-218)
Kokelj S V, Lacelle D, Lantz T C, Tunnicliffe J, Malone L, Clark I D and Chin K S 2013 Thawing of massive ground ice in mega slumps drives increases in stream sediment and solute flux across a range of watershed scales *J. Geophys. Res.* **118** 681–92
Kokelj S V, Lantz T C, Kanigan J, Smith S L and Coutts R 2009 Origin and polycyclic behaviour of tundra thaw slumps, Mackenzie Delta region, Northwest Territories, Canada *Permafrost Periglacial Process.* **20** 173–84
Kokelj S V, Lantz T C, Tunnicliffe J, Segal R and Lacelle D 2017a Climate-driven thaw of permafrost preserved glacial landscapes, northwestern Canada *Geology* **45** 371–4
Kokelj S V, Smith C A S and Burn C R 2002 Physical and chemical characteristics of the active layer and permafrost, Herschel Island, western Arctic Coast, Canada *Permafrost Periglacial Process.* **13** 171–85
Kokelj S V, Tunnicliffe J F and Lacelle D 2017b The peel plateau of Northwestern Canada: an ice-rich hummocky moraine landscape in transition *Landscapes and Landforms of Western Canada* ed O Slaymaker (Berlin: Springer) 109–22
Kokelj S V, Tunnicliffe J, Lacelle D, Lantz T C, Chin K S and Fraser R 2015 Increased precipitation drives mega slump development and destabilization of ice-rich permafrost terrain, northwestern Canada *Glob. Planet Change* **129** 56–68
Lacelle D, Bjornson J, Lauriol B, Clark I D and Troutet Y 2004 Segregated-intrusive ice of subglacial meltwater origin in retrogressive thaw flow headwalls, Richardson Mountains, NWT, Canada *Quat. Sci. Rev.* **23** 681–96
Lacelle D, Fontaine M, Pellerin A, Kokelj S V and Clark I D 2019 Legacy of holocene landscape changes on soil biogeochemistry: a perspective from paleo-active layers in Northwestern Canada *J. Geophys. Res.* **124** 2662–79
Lacelle D, Lauriol B, Zazula G, Ghaleb B, Utting N and Clark I D 2013 Timing of advance and basal condition of the Laurentide Ice Sheet during the last glacial maximum in the Richardson Mountains *NWT Quat. Res.* **80** 274–83
Lamoureux S F and Lafrenière M J 2014 Seasonal fluxes and age of particulate organic carbon exported from Arctic catchments impacted by localized permafrost slope disturbances *Environ. Res. Lett.* **9** 045002
Lane L, Roots C and Fraser T 2012 *Geology Herschel Island Qikiqtaryuk: A Natural and Cultural History of Yukon's Arctic Island*, ed C Burn (Calgary: University of Calgary Press)
Lenth R V 2016 Least-squares means: the R package lsmeans *J. Stat. Softw.* **69** 1–33
Levenstein B, Culp J M and Lento J 2018 Sediment inputs from retrogressive thaw slumps drive algal biomass accumulation but not decomposition in Arctic streams, NWT *Freshw. Biol.* **63** 1300–15
Lewkowicz A G and Way R G 2019 Extremes of summer climate trigger thousands of thermokarst landslides in a High Arctic environment *Nat. Commun.* **10** 1–11
Littlefair C A and Tank S E 2018 Biodegradability of thermokarst carbon in a till-associated, glacial margin landscape: the case of the peel plateau, NWT, Canada *J. Geophys. Res.* **123** 3293–307
Littlefair C A, Tank S E and Kokelj S V 2017 Retrogressive thaw slumps temper dissolved organic carbon delivery to streams of the Peel Plateau, NWT, Canada *Biogeosciences* **14** 5487–505
Ma S, Chen Y, Lu X and Wang X 2018 1Soil organic matter chemistry: based on pyrolysis-gas chromatography- mass spectrometry (Py-GC/MS) *Mini Rev. Org. Chem.* **15** 389–403
Malone L, Lacelle D, Kokelj S and Clark I D 2013 Impacts of hillslope thaw slumps on the geochemistry of permafrost catchments (Stony Creek watershed, NWT, Canada) *Chem. Geol.* **356** 38–49
Mann P J *et al* 2014 Evidence for key enzymatic controls on metabolism of Arctic river organic matter *Glob. Change Biol.* **20** 1089–100
Manning D W P, Rosemond A D, Kominoski J S, Gulis V, Benstead J P and Maerz J C 2015 Detrital stoichiometry as a critical nexus for the effects of streamwater nutrients on leaf litter breakdown rates *Ecology* **96** 2214–24
Mccallister S L, Ishikawa N F and Kothawala D N 2018 Biogeochemical tools for characterizing organic carbon in inland aquatic ecosystems *Limnol. Oceanogr. Lett.* **3** 444–57
Mcclelland J W *et al* 2016 Particulate organic carbon and nitrogen export from major Arctic rivers *Glob. Biogeochem. Cycles* **30** 2015GB005351
Moorhead D L and Sinsabaugh R L 2006 A theoretical model of litter decay and microbial interaction *Ecol. Monogr.* **76** 151–74
Murphy K R, Stedmon C A, Graeber D and Bro R 2013 Fluorescence spectroscopy and multi-way techniques. PARAFAC *Anal. Methods* **5** 6557
Murphy K R, Stedmon C A, Wenig P and Bro R 2014 OpenFluor– an online spectral library of auto-fluorescence by organic compounds in the environment *Anal. Methods* **6** 658–61
Murton J B and Ballantyne C K 2017 Chapter 5 Periglacial and permafrost ground models for Great Britain *Geol. Soc. London Eng. Geol. Spec. Publ.* **28** 501–97
Norris D K 1985 *Geology of the Northern Yukon and Northwestern District of Mackenzie* (Ottawa: Geological Survey of Canada) "A" Series Map 1581A
Olefeldt D *et al* 2016 Circumpolar distribution and carbon storage of thermokarst landscapes *Nat. Commun.* **7** 13043
Osburn C L, Handsel L T, Mikan M P, Paerl H W and Montgomery M T 2012 Fluorescence tracking of dissolved and particulate organic matter quality in a river-dominated estuary *Environ. Sci. Technol.* **46** 8628–36
O'Neill H B, Burn C R, Kokelj S V and Lantz T C 2015 'Warm' tundra: atmospheric and near-surface ground temperature inversions across an alpine treeline in continuous

permafrost, Western Arctic, Canada: near-surface ground temperatures across an alpine treeline *Permafrost Periglacial Process.* **26** 103–18
Panneer Selvam B, Lapierre J-F, Guillemette F, Voigt C, Lamprecht R E, Biasi C, Christensen T R, Martikainen P J and Berggren M 2017 Degradation potentials of dissolved organic carbon (DOC) from thawed permafrost peat *Sci. Rep.* **7** 1–9
Pautler B G, Simpson A J, Mcnally D J, Lamoureux S F and Simpson M J 2010 Arctic permafrost active layer detachments stimulate microbial activity and degradation of soil organic matter *Environ. Sci. Technol.* **44** 4076–82
Peter S, Isidorova A and Sobek S 2016 Enhanced carbon loss from anoxic lake sediment through diffusion of dissolved organic carbon *J. Geophys. Res.* **121** 1959–77
Plaza C *et al* 2019 Direct observation of permafrost degradation and rapid soil carbon loss in tundra *Nat. Geosci.* **12** 627–31
Ramage J L, Irrgang A M, Morgenstern A and Lantuit H 2018 Increasing coastal slump activity impacts the release of sediment and organic carbon into the Arctic Ocean *Biogeosciences* **15** 1483–95
Richardson D C, Newbold J D, Aufdenkampe A K, Taylor P G and Kaplan L A 2013 Measuring heterotrophic respiration rates of suspended particulate organic carbon from stream ecosystems: measuring respiration rates of POC *Limnol. Oceanogr. Methods* **11** 247–61
Roiha T, Peura S, Cusson M and Rautio M 2016 Allochthonous carbon is a major regulator to bacterial growth and community composition in subarctic freshwaters *Sci. Rep.* **6** 1–12
Rudy A C A, Lamoureux S F, Kokelj S V, Smith I R and England J H 2017 Accelerating thermokarst transforms ice-cored terrain triggering a downstream cascade to the ocean *Geophys. Res. Lett.* **44** 080–11
Sardans J, Rivas-Ubach A and Peñuelas J 2012 The elemental stoichiometry of aquatic and terrestrial ecosystems and its relationships with organismic lifestyle and ecosystem structure and function: a review and perspectives *Biogeochemistry* **111** 1–39
Schimel J P and Weintraub M N 2003 The implications of exoenzyme activity on microbial carbon and nitrogen limitation in soil: a theoretical model *Soil Biol. Biochem.* **35** 549–63
Schirrmeister L, Froese D, Tumskoy V, Grosse G, Wetterich S*et al* 2013 *Permafrost And Periglacial Features | Yedoma: Late Pleistocene Ice-Rich Syngenetic Permafrost of Beringia Encyclopedia of Quaternary Science*, ed S Elisa and C Mock (Amsterdam: Elsevier) pp 542–52
Schubert C J and Calvert S E 2001 Nitrogen and carbon isotopic composition of marine and terrestrial organic matter in Arctic Ocean sediments:: implications for nutrient utilization and organic matter composition *Deep Sea Res. Part I* **48** 789–810
Segal R A, Lantz T C and Kokelj S V 2016 Acceleration of thaw slump activity in glaciated landscapes of the Western Canadian Arctic *Environ. Res. Lett.* **11** 034025
Sinsabaugh R L and Follstad Shah J J 2012 Ecoenzymatic Stoichiometry and Ecological Theory *Annu. Rev. Ecol. Evol. Syst.* **43** 313–43
Sinsabaugh R L and Follstad Shah J J 2011 Ecoenzymatic stoichiometry of recalcitrant organic matter decomposition: the growth rate hypothesis in reverse *Biogeochemistry* **102** 31–43
Sinsabaugh R L and Follstad Shah J J 2010 Integrating resource utilization and temperature in metabolic scaling of riverine bacterial production *Ecology* **91** 1455–65
Sinsabaugh R L, Manzoni S, Moorhead D L and Richter A 2013 Carbon use efficiency of microbial communities: stoichiometry, methodology and modelling *Ecol. Lett.* **16** 930–9
Slaymaker O and Kovanen D J 2017 Long-term geomorphic history of Western Canada *Landscapes and Landforms of Western Canada World Geomorphological Landscapes* ed O Slaymaker (Berlin: Springer) 3–26
Spencer R G M, Mann P J, Dittmar T, Eglinton T I, Mcintyre C, Holmes R M, Zimov N and Stubbins A 2015 Detecting the signature of permafrost thaw in Arctic rivers *Geophys. Res. Lett.* **42** 2830–5
Stelzer R S, Heffernan J and Likens G E 2003 The influence of dissolved nutrients and particulate organic matter quality on microbial respiration and biomass in a forest stream *Freshw. Biol.* **48** 1925–37
Stock B C, Jackson A L, Ward E J, Parnell A C, Phillips D L and Semmens B X 2018 Analyzing mixing systems using a new generation of Bayesian tracer mixing models *Peer J.* **6** e5096
Strauss J *et al* 2017 Deep Yedoma permafrost: A synthesis of depositional characteristics and carbon vulnerability *Earth Sci. Rev.* **172** 75–86
Stubbins A, Lapierre J-F, Berggren M, Prairie Y T, Dittmar T and Del Giorgio P A 2014 What's in an EEM? Molecular signatures associated with dissolved organic fluorescence in Boreal Canada *Environ. Sci. Technol.* **48** 10598–606
Tank S E, Vonk J E, Walvoord M A, Mcclelland J W, Laurion I and Abbott B W 2020 Landscape matters: predicting the biogeochemical effects of permafrost thaw on aquatic networks with a state factor approach *Permafrost Periglacial Process.* **31** 358–70
Tanski G, Lantuit H, Ruttor S, Knoblauch C, Radosavljevic B, Strauss J, Wolter J, Irrgang A M, Ramage J and Fritz M 2017 Transformation of terrestrial organic matter along thermokarst-affected permafrost coasts in the Arctic *Sci. Total Environ.* **581–582** 434–47
Tanski G, Wagner D, Knoblauch C, Fritz M, Sachs T and Lantuit H 2019 Rapid CO_2 release from eroding permafrost in seawater *Geophys. Res. Lett.* **46** 11244–52
Turetsky M R *et al* 2020 Carbon release through abrupt permafrost thaw *Nat. Geosci.* **13** 138–43
Vonk J E *et al* 2012 Activation of old carbon by erosion of coastal and subsea permafrost in Arctic Siberia *Nature* **489** 137–40
Vonk J E *et al* 2013 High biolability of ancient permafrost carbon upon thaw *Geophys. Res. Lett.* **40** 2689–93
Vonk J E *et al* 2015 Reviews and syntheses: effects of permafrost thaw on Arctic aquatic ecosystems *Biogeosciences* **12** 7129–67
Ward C P and Cory R M 2015 Chemical composition of dissolved organic matter draining permafrost soils *Geochim. Cosmochim. Acta* **167** 63–79
Ward Jones M K , Pollard W H and Jones B M 2019 Rapid initialization of retrogressive thaw slumps in the Canadian high Arctic and their response to climate and terrain factors *Environ. Res. Lett.* **14** 055006
Wauthy M, Rautio M, Christoffersen K S, Forsström L, Laurion I, Mariash H L, Peura S and Vincent W F 2018 Increasing dominance of terrigenous organic matter in circumpolar freshwaters due to permafrost thaw *Limnol. Oceanogr. Lett.* **3** 186–98
Welti N *et al* 2017 Bridging food webs, ecosystem metabolism, and biogeochemistry using ecological stoichiometry theory *Front. Microbiol.* **8** 1298
Wickland K P, Waldrop M P, Aiken G R, Koch J C, Jorgenson M T and Striegl R G 2018 Dissolved organic carbon and nitrogen release from boreal Holocene permafrost and seasonally frozen soils of Alaska *Environ. Res. Lett.* **13** 065011
Wild B, Andersson A, Bröder L, Vonk J, Hugelius G, Mcclelland J W, Song W, Raymond P A and Gustafsson Ö 2019 Rivers across the Siberian Arctic unearth the patterns of carbon release from thawing permafrost *Proc Natl Acad. Sci.* **116** 10280–5
Zazula G D, Mackay G, Andrews T D, Shapiro B, Letts B and Brock F 2009 A late Pleistocene steppe bison (Bison priscus) partial carcass from Tsiigehtchic, Northwest Territories, Canada *Quat. Sci. Rev.* **28** 2734–42
Zolkos S and Tank S E 2020 Experimental evidence that permafrost thaw history and mineral composition shape

abiotic carbon cycling in thermokarst-affected stream networks *Front. Earth Sci.* **8** 152

Zolkos S, Tank S E and Kokelj S V 2018 Mineral weathering and the permafrost carbon-climate feedback *Geophys. Res. Lett.* **45** 9623–32

Zolkos S and Tank S E 2019 Permafrost geochemistry and retrogressive thaw slump morphology (Peel Plateau, Canada), v. 1.0 (2017-2017). Nordicana D45 (https://doi.org/10.5885/45573XD-28DD57D553F14BF0)

Zolkos S, Tank S E, Striegl R G and Kokelj S V 2019 Thermokarst effects on carbon dioxide and methane fluxes in streams on the peel plateau (NWT, Canada) *J. Geophys. Res.* **124** 1781–98

van der Sluijs J, Kokelj S V, Fraser R H, Tunnicliffe J and Lacelle D 2018 Permafrost Terrain Dynamics and Infrastructure Impacts Revealed by UAV Photogrammetry and Thermal Imaging *Remote Sens.* **10** 1734